e-Polymers **2009**, no. 030

http://www.e-polymers.org

ISSN 1618-7229

Application of the Monte Carlo simulation method to the Investigation of the effect of chain-length-dependent bimolecular termination on ATRP

Mohammad Najafi,[1] *Vahid Haddadi-Asl,*[1*] *Mehdi Salami-Kalajahi,*[1] *Hossein Roughani Mamaghani*[1]

[1]Polymer Engineering Department, Amirkabir University of Technology, P.O. Box 15875-4413, Tehran, Iran; fax: +98 21 88037433; e-mails: m.najafi@aut.ac.ir, haddadi@aut.ac.ir, mskalajahi@aut.ac.ir, r.mamaghani@aut.ac.ir;

(Received: 28 June, 2008; published: 21 March, 2009)

Abstract: An optimized and high-performance Monte Carlo simulation is developed to take thorough account of the influence of chain-length-dependent termination rate constant on polymer microstructure in ATRP. According to the simulation results, bimolecular termination rate constant sharply drops throughout the polymerization when chain length dependency is applied to the program. The dependence of $ln\left(\frac{M_0}{M}\right)$ on reaction time, as a common feature of ATRP, is almost linear. Moreover, the polymerization proceeds to higher conversion when the chain-length-dependent termination rate constant is applied to the simulation model. In addition, the plot of $ln\left(\frac{I_0}{I}\right)$ against reaction time is completely linear; also, the initiator is entirely decomposed at the early stages of the polymerization as the plot of C_I against time shows. The concentration of the catalyst in lower oxidation state decreases first and then plateaus at higher conversion. Furthermore, the amount of $M_t^n Y/L$ used in the polymerization is lower when the chain-length-dependent termination rate constant is employed in the simulation. Finally, the peak of molecular weight distribution of polymer chains shifts toward higher molecular weight during the reaction. Besides, the molecular weight distribution broadens at higher conversion. However, the molecular weight distribution of polymer chains produced under conditions of applying chain-length-dependent termination rate constant is narrower.

Keywords: Controlled/"Living" Radical Polymerization, Monte Carlo Simulation, Molecular Weight Distribution, Polydispersity Index.

Introduction

In the recent years, various attempts have been made to apply control over free radical polymerization by using different procedures, which are mainly supposed to control the reactions between two free radical species. To this end, versatile methods—known as controlled/"living" radical polymerizations—have been developed to combine the versatility of free radical polymerization with the controlling features of living anionic polymerization. Having brought chain structure under control, this new concept has provided new and advanced applications of free radical polymerization techniques [1-6].

The key kinetic feature of all these methods is the reduction of termination/transfer reactions by reducing the concentration of free radical species during the reaction through a dynamic activation/deactivation cycle. In other words, growing chains switch between active and dormant states so as to drop the instantaneous concentration of free radicals and thereby suppressing the bimolecular termination reaction rates which are normally related to the square of radical concentration [7].

Of the various controlled polymerizations, nitroxide-mediated polymerization (NMP) [8–10], reversible addition-fragmentation chain transfer (RAFT) [11, 12], and atom-transfer radical polymerization (ATRP) [13, 14] are known as the most common techniques. The latter, which is founded on the reversible termination of radical species, has attracted more attention due its simplicity and its more similarity to the conventional free radical polymerization. It utilizes a transition metal complex as the medium of halogen atom transfer to change a growing radical into a dormant species (Scheme 1).

Scheme 1. Equilibrium of ATRP Reaction.

To inspect the behavior of ATRP, several analytical models and mathematical modeling have been introduced. For instance, moment equations have been successfully employed to predict the molecular weight averages of living free radical polymerizations [15-24]. However, they are not able to predict molecular weight distributions. The PREDICI has also been used as a powerful tool to solve a series of differential equations so as to obtain full molecular weight distributions of macromolecules produced by different living free radical polymerizations [25-30]. In addition, Monte Carlo method, owing to the statistical nature of the chain growth and chain terminating reactions, is another excellent method utilized to simulate both conventional free radical (co)polymerization systems [31-33] and controlled free radical polymerizations [34-40]. Monte Carlo method overweighs other analytical methods in several ways: for example, it can be easily implemented to different polymerization systems. In addition, compared to moment equations, it is not restricted to solving stiff differential equations. Moreover, it does not require stringent assumptions which mainly cause most of analytical methods to lead to approximate results. Furthermore, Monte Carlo method is capable of storing the whole information of polymer chains while the reaction proceeds, and therefore, it can compute the rates of different reactions (such as activation, deactivation, propagation, transfer, etc.), the concentration of reaction components, and molecular weight averages in the course of the polymerization. Finally, it can visualize the detailed chain length distributions of the macromolecules virtually synthesized. Nonetheless, unfortunately, inefficient simulation programs based on Monte Carlo method usually take long times to complete, if not implemented properly.

To the best knowledge of the authors, a review of related literature indicates that the Monte Carlo simulations of ATRP—and particularly ATRP of styrene—presented so

far [37, 41] have mainly dealt with the common reactions such as equilibrium, propagation, termination, and transfer and have not taken the chain end degradation reactions into consideration as shown in

Scheme 2. These reactions, by reason of dealing with the catalyst in higher oxidation state, can have a great impact on the role of the catalyst as the regulating agent of ATRP and thereby influencing the living nature of the polymerization. Moreover, presented simulations have ignored the effect of chain length on termination rate constant, which can affect the contribution of termination reaction and thereby the livingness of the reaction.

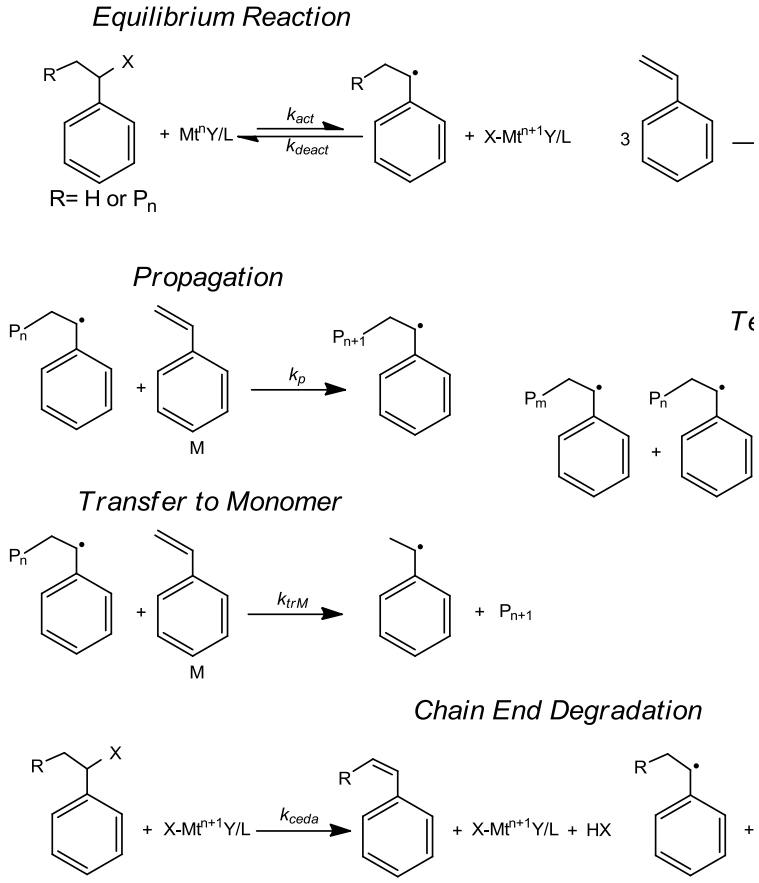

Scheme 2. Simulation Reactions of ATRP of styrene.

In this contribution, Monte Carlo method is applied to the controlled free radical polymerization by employing a thorough kinetic scheme including chain end degradation reactions [42]. Additionally, we investigate the effect of chain-length-dependent termination rate constant on polymer properties, namely molecular weight distributions of chains, in our simulation. Conversion; reactant concentration; molecular weight averages; and molar and weight chain length distributions are also considered as the response parameters of the simulation.

Simulation Description

The kinetic scheme used in the simulation includes activation, deactivation, thermal initiation, propagation, termination by combination, transfer to monomer, and chain

end degradation reactions [42]. The elementary reaction steps of ATRP used in the simulation are listed in Equations (1) to (9). The kinetic parameters and initial concentrations inputted to the simulation are also given in

Tab. 1.

$$RX + M_t^n Y/L \xrightarrow{k_{act}} R^\bullet + X\text{-}M_t^{n+1} Y/L \quad (1)$$

$$3M \xrightarrow{k_{therm}} R^\bullet + R'^\bullet \quad (2)$$

$$R^\bullet + X\text{-}M_t^{n+1} Y/L \xrightarrow{k_{deact}} RX + M_t^n Y/L \quad (3)$$

$$P_n X + M_t^n Y/L \xrightarrow{k_{act}} P_n^\bullet + X\text{-}M_t^{n+1} Y/L \quad (4)$$

$$P_n^\bullet + M \xrightarrow{k_p} P_{n+1}^\bullet \quad (5)$$

$$P_n^\bullet + M \xrightarrow{k_{trM}} P_{n+1} + R^\bullet \quad (6)$$

$$P_m^\bullet + P_n^\bullet \xrightarrow{k_{tc}} P_{m+n} \quad (7)$$

$$P_n X + X\text{-}M_t^{n+1} Y/L \xrightarrow{k_{ceda}} P_n + X\text{-}M_t^{n+1} Y/L + HX \quad (8)$$

$$P_n^\bullet + X\text{-}M_t^{n+1} Y/L \xrightarrow{k_{cedb}} P_n + M_t^n Y/L + HX \quad (9)$$

Tab. 1. Kinetic rate constants and initial concentrations used in simulation of styrene ATRP at 110 °C.

Coefficient/Parameter	Expression/Value	Reference
k_{act} (L.mol^{-1}.s^{-1})	0.45	[43, 45]
k_{therm} (L^2.mol^{-2}.s^{-1})	2.19×10^5 exp(-13800 K/*T*)	[44]
k_{deact} (L.mol^{-1}.s^{-1})	1.1×10^7	[45]
k_p (L.mol^{-1}.s^{-1})	4.266×10^7 exp(-3910 K/*T*)	[44]
k_{tc}^0 (L.mol^{-1}.s^{-1})	3.82×10^9 exp(-958 K/*T*)	[44]
k_{trM} (L.mol^{-1}.s^{-1})	2.31×10^6 exp(-6377 K/*T*)	[44]
k_{ceda} (L.mol^{-1}.s^{-1})	1.0×10^{-4}	[46]
k_{cedb} (L.mol^{-1}.s^{-1})	1.63×10^3	[42]
$[M]_0$ (mol.L^{-1})	1	this work
$[RX]_0$ (mol.L^{-1})	0.01	this work
$[M_t^n Y/L]_0$ (mol.L^{-1})	0.01	this work

To consider the effect of chain length on bimolecular termination reaction rates, different models have been proposed; given herein is a composite model used to calculate the termination rate constant of two radicals with lengths of *i* and *j*, i.e. $k_{tc}^{i,j}$, based on the termination rate constant of two homo-length radicals ($k_{tc}^{i,i}$) [47-51]. It is proposed that "short" radicals of the same length terminate with each other according to the following standard functional form:

$$k_{tc}^{i,i}\left(\frac{L}{mol.s}\right) = k_{tc}^0 \times i^{-e_S}; \quad i \le i_c \quad (10)$$

This k_{tc}^{0} should be the real rate coefficient for termination between two monomeric free radicals. *i* and i_c are respectively the chain length and the critical chain length indicating the short length boundary; e_s is also equal to 0.5 [51].

However, for "long" radicals the following equation is proposed:

$$k_{tc}^{i,i}\left(\frac{L}{mol.s}\right) = k_{tc}^{0} \times \ i_c \ ^{-e_S+e_L} \times i^{-e_L}; \ \ i > i_c \tag{11}$$

where, the $k_{tc}^{0} \times (i_c)^{-e_S+e_L}$ term in this equation gives continuity with Equation (10) at the "crossover" chain length (i_c); e_L and i_c are reported to be equal to 0.16 and 100 respectively [51]. To summarize, we use the following composite model in this paper:

$$\begin{aligned} k_{tc}^{i,i}\left(\frac{L}{mol.s}\right) &= k_{tc}^{0} \times i^{-0.5}; \ \ i \le i_c \\ k_{tc}^{i,i}\left(\frac{L}{mol.s}\right) &= k_{tc}^{0} \times \ i_c \ ^{-0.34} \times i^{-0.16}; \ \ i > i_c \end{aligned} \tag{12}$$

To specify values of the cross-termination rate coefficients ($k_{tc}^{i,j}$), where $i \neq j$, three commonly used models are based on harmonic, diffusion, and geometric means as summarized below:

$$\begin{aligned} k_{tc}^{i,j} \ \ hm \ \left(\frac{L}{mol.s}\right) &= k_{tc}^{0} \times \left(\frac{2ij}{i+j}\right)^{-0.5} \ ; \ \ i \le i_c \\ k_{tc}^{i,j} \ \ hm \ \left(\frac{L}{mol.s}\right) &= k_{tc}^{0} \times \ i_c \ ^{-0.34} \times \left(\frac{2ij}{i+j}\right)^{-0.16} \ ; \ \ i > i_c \end{aligned} \tag{13}$$

$$k_{tc}^{i,j} \ \ dm \ \left(\frac{L}{mol.s}\right) = 0.5 \times \ k_{tc}^{i,i} + k_{tc}^{j,j} \tag{14}$$

$$k_{tc}^{i,j} \ \ gm \ \left(\frac{L}{mol.s}\right) = \sqrt{k_{tc}^{i,i} \times k_{tc}^{j,j}} \tag{15}$$

The overall rate coefficient for termination—the termination rate coefficient observed in a conventional free radical polymerization—at any instant of the polymerization can be correlated to $k_{tc}^{i,j}$ constants (either diffusion, geometric or harmonic mean) as reads:

$$\overline{k_{tc}}\left(\frac{L}{mol.s}\right) = \sum_{i=1}^{\infty}\sum_{j=1}^{\infty} k_{tc}^{i,j} \frac{[R_i] \times [R_j]}{[R] \times [R]} \tag{16}$$

where, $[R_i]$ and $[R_j]$ stand for the concentration of chains with the length of *i* and *j* respectively. [R] is also the total concentration of all radical species. As this statement implies, Equation (16) is not also restricted to steady states. Because the termination nature is similar in both conventional free radical polymerization and atom transfer radical polymerization, the same model is adopted for ATRP in our simulation. It is also assumed that the rate constants are not diffusion-controlled in the course of the simulation.

The Monte Carlo methodology employed herein is adopted from the well-known Gillespie's algorithm [52]. A simulation volume equal to 1×10^{-14} liters is considered to calculate the number of different reactants based on their concentrations and to transform the experimental reaction rate constants into stochastic rate constants as required in the Gillespie's algorithm. As a result, taking into account that the concentration of initiator is 0.01 ($mol.L^{-1}$), 6.023×10^{7} chains are theoretically synthesized during the simulation program. However, it should be born in mind that some more chains are also created by thermal initiation of monomer. A schematic representation of the simulation algorithm is portrayed in

Scheme 3.

A subroutine on the base of improved Mersenne Twister algorithm is used in the simulation to produce random numbers with long period lengths—which is required to avoid the repetition of random numbers in polymerization reactions. This subroutine is written in C++ language and the generated random numbers satisfy the tests of uniformity and serial correlation with high resolution. It should also be noted that the cycle length of this random number generator is long enough, namely 2^{216091}-1, to cover the needs of this simulation. A suitable and optimized program according to the flow chart presented in

Scheme 3 is written in C++ language and compiled on a 64-bit openSuSE Linux operating system to manage the huge amount of memory requested by the program. The average run time of the program for a simulation volume of 1×10^{-14} liters on a computer equipped with two 2.0 GHz CPU's and 4 GB memory is approximately 2 hours.

Results and Discussion

It is highly asserted that as macromolecules become longer, due to hindrance effects and lower mobility of chains, the bimolecular termination rates decrease. In other words, the bimolecular termination rates between macromolecules are almost an order of magnitude smaller than those of monomeric species. The model employed herein is based on a composite model that considers a critical chain length around which the dependency of termination rate constant on chain length is calculated by using two different equations. In addition, three models based on diffusion, geometric, and harmonic means are used to calculate the cross-termination rate constants.

Simulating Bimolecular Termination Rate Constant

Fig. 1 shows the variation of these three mean values as a function of reaction time. As it can be seen, all the three models, namely diffusion, geometric, and harmonic means, lead to the similar results. Moreover, the cross-termination rate constants given by three models decrease as the reaction proceeds. In effect, since in controlled/"living" free radical polymerization the molecular weight of chains rises over the course of the polymerization, the chain-length-dependent bimolecular termination rate constants fall accordingly and finally level off. Therefore, it can be inferred that the dependency of bimolecular termination rate constants on chain length is mainly controlled by a certain chain length beyond which the mobility, and

consequently reactivity, of radical chains remains constant, and thus no more decrease in the rate constants is seen. Since all the three models have ended in similar trends, to avoid extra computation, only geometric model is applied to the simulation program.

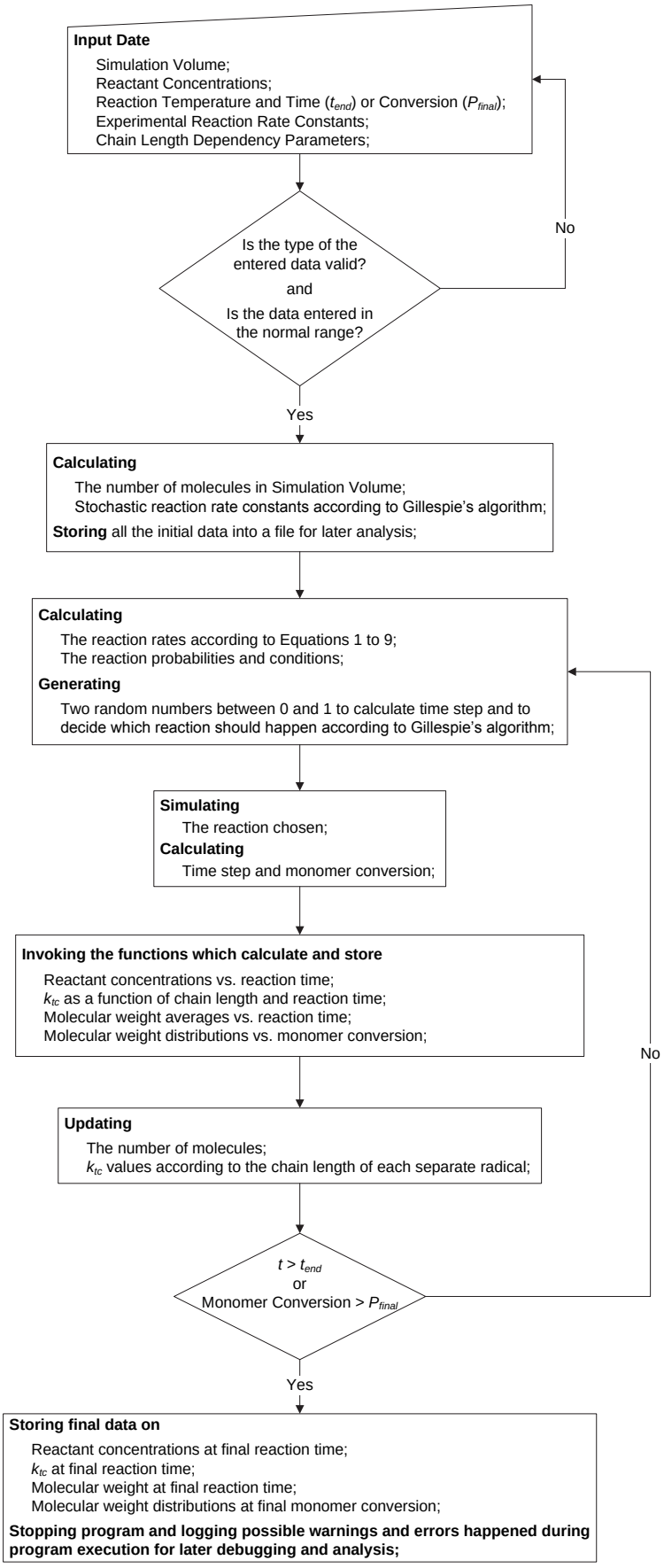

Scheme 3. The simulation algorithm of ATRP of Styrene

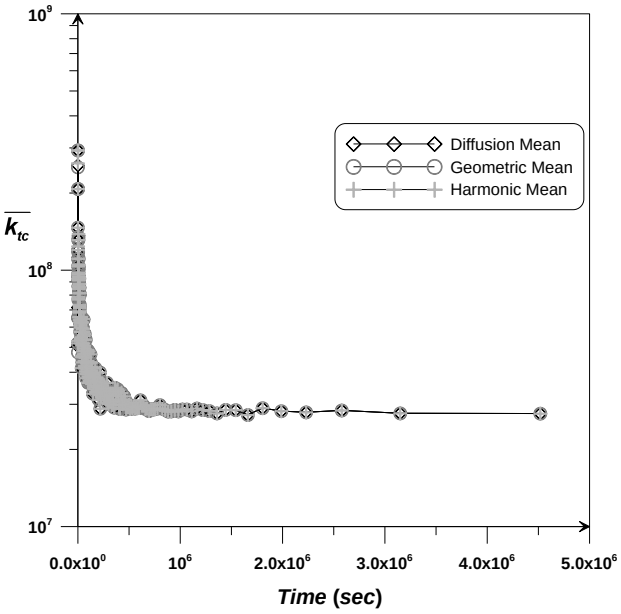

Fig. 1. The chain-length-dependent bimolecular termination rate constant as a function of reaction time.

Simulating Dependence of Reactants on Reaction Time

The variation of monomer conversion in terms of $ln\left(\frac{M_0}{M}\right)$ versus reaction time is depicted in

Fig. 2. In accordance with the results, $ln\left(\frac{M_0}{M}\right)$ grows linearly at the initial stages of the reaction; however, due to termination reactions, at the final stages of the polymerization the $ln\left(\frac{M_0}{M}\right)$ curves start dropping and deviating from linearity.

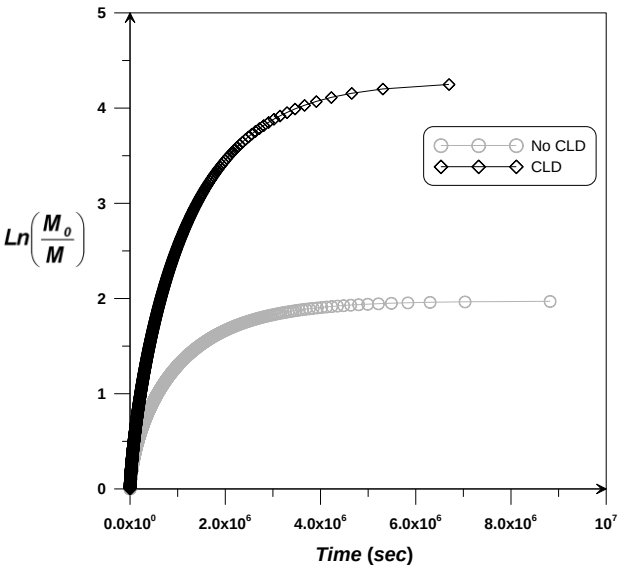

Fig. 2. Illustration of the dependence of $ln\left(\frac{M_0}{M}\right)$ on reaction time

Moreover, including chain length dependency of termination rate, as represented by "CLD" legend in all figures henceforth, changes the trend of monomer conversion; actually, owing to smaller termination rate constant, the reaction proceeds to higher conversion (98.5%) when bimolecular termination rates are computed with having taken into account the chain length effect. In fact, as the amount of bimolecular termination reactions decreases, the polymer radicals can further maintain their livingness during the reaction. On the other hand, when termination rate constants are not chain-length dependent, as represented by "No CLD" legend in all figures henceforth, the reaction stops before completion at conversion about 86%.

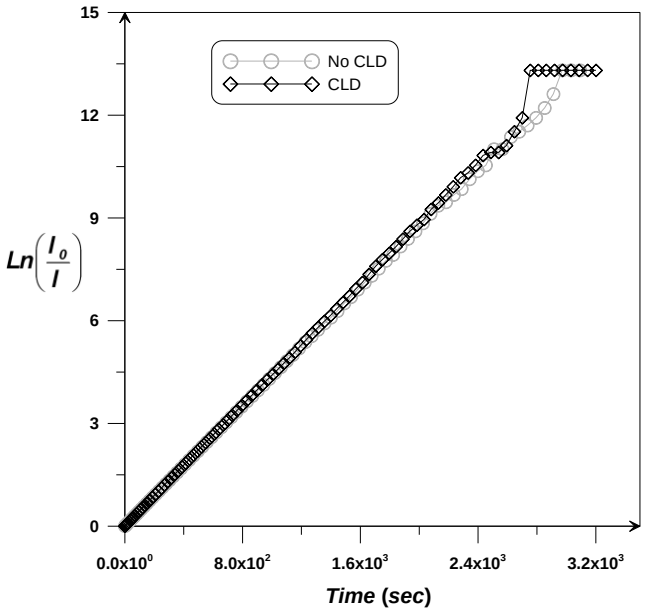

Fig. 3. Illustration of the dependence of $ln\left(\frac{I_0}{I}\right)$ on reaction time.

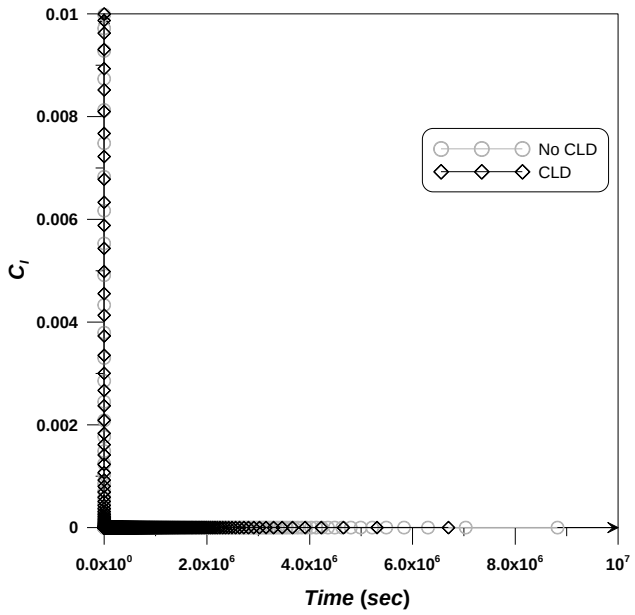

Fig. 4. Change in the concentration of initiator.

As another case in point, the variation of $ln\left(\frac{I_0}{I}\right)$ versus reaction time is represented in Fig. 3. The change in the concentration of initiator over the course of the polymerization reaction is also delineated in

Fig. 4. It is obvious that, thanks to fast initiation, initiator is entirely decomposed at the very early stages of the polymerization. It should also be noticed that the same results are obtained regardless of the effect of chain length on termination rate constant since initiator is completely consumed in the activation process without being affected by termination or transfer reactions.
Fig. 5 and Fig. 6 show the dependence of catalysts in lower oxidation state, namely M_t^nY/L, and in higher oxidation state, that is $X\text{-}M_t^{n+1}Y/L$, respectively. According to Fig. 5, the concentration of M_t^nY/L decreases as the reaction progresses and finally reaches a plateau. Since the progress of the polymerization gives rise to radical termination, albeit so small, the concentration of growing radicals drops, which correspondingly shifts the equilibrium toward the formation of new growing radicals and thereby consuming more of M_t^nY/L. Besides, it is obvious that the concentration of M_t^nY/L is higher when the effect of chain length on termination rate constant is taken into consideration. In fact, because of smaller bimolecular termination rate constant in this case, less bimolecular termination happens and consequently the concentration of growing radicals decreases much less. Therefore, a smaller amount of M_t^nY/L is used before it plateaus.

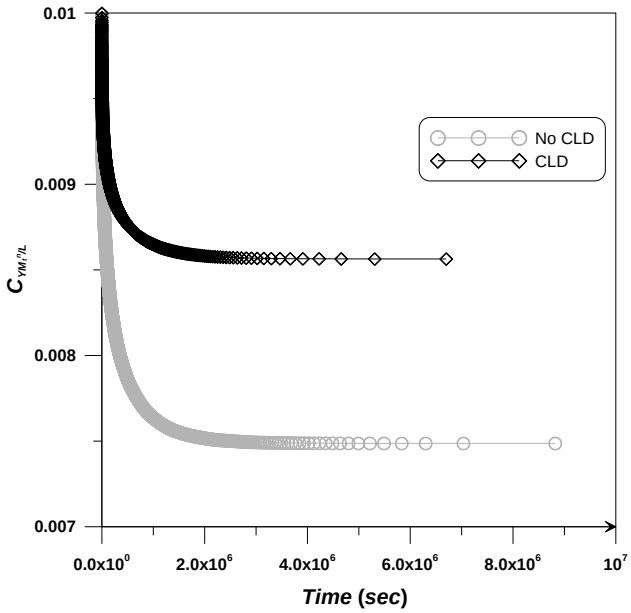

Fig. 5. Change in $\mathbf{M_t^nY/L}$ concentration.

On the other hand, the concentration of $X\text{-}M_t^{n+1}Y/L$ increases as the polymerization reaction progresses and finally levels out. By reason of termination reactions

available in the system—and thus the irreversible termination of growing radicals—the equilibrium reaction in ATRP tends to move toward the activation of dormant chains and the production of new radicals; ergo, contrary to $M_t^n Y/L$, the concentration of $X\text{-}M_t^{n+1}Y/L$ increases at the early stages of the reaction and finally reaches a plateau since termination reactions abate at higher conversion. Moreover, in case of considering the effect of chain length on termination rate constant, the concentration of $X\text{-}M_t^{n+1}Y/L$ is much smaller, which represents less accumulation of catalyst in higher oxidation state. Indeed, as a result of smaller termination rate constant in this case, less growing radicals terminate, and therefore less $X\text{-}M_t^{n+1}Y/L$ is built up.

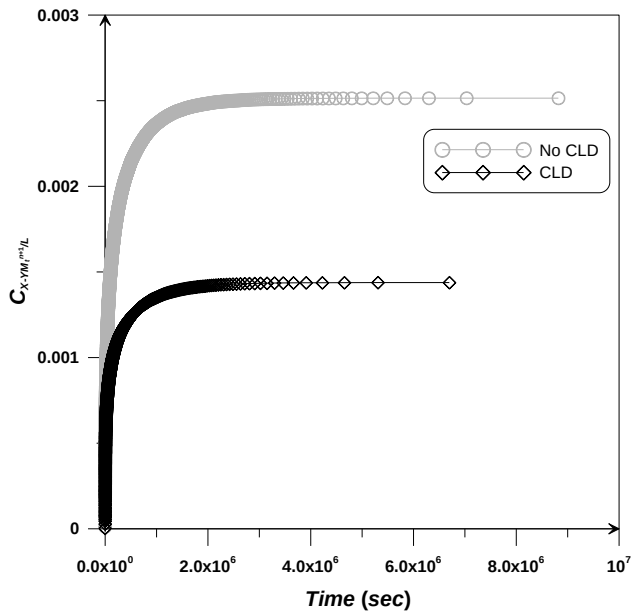

Fig. 6. Change in $\mathbf{X\text{-}M_t^{n+1}Y/L}$ concentration.

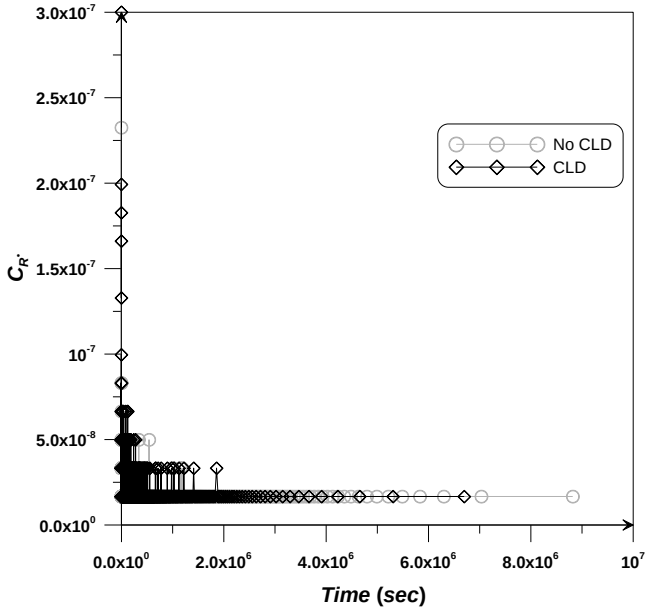

Fig. 7. Change in the concentration of growing radicals.

Fig. 7 portrays the dependence of growing radicals on reaction time. As depicted in this figure, the concentration of growing radicals, regardless of the initial stage of the polymerization, is almost constant. Moreover, the unnatural fluctuations (particularly at the beginning of the polymerization) in curves are attributed to the unsteadiness of the polymerization—and in particular equilibrium reaction. In fact, since the concentration of free radicals in ATRP systems, compared to FRP ones, is much lower, a small change in the reaction may result in noticeable fluctuations. It is also clear that the chain length effect on termination reaction does not significantly affect the concentration of growing radicals since—because of equilibrium reaction and living nature of ATRP—it is already reduced to very small amounts.

Simulating Dependence of Molecular Weight and Polydispersity Index on Reaction Time

The living nature of ATRP has successfully fulfilled the requirements of producing tailor-made polymers with narrow molecular weight distribution. It also provides the prerequisites for obtaining molecular weight that linearly augments over the course of the polymerization. To monitor the effect of chain-length-dependent bimolecular termination rate constant on polymer properties, Monte Carlo simulation method is utilized to calculate the change in number-, weight-, and z-average molecular weights as the polymerization progresses. Furthermore, the program is optimized to simulate the polymerization system so that the molecular weight of generated polymer chains lies in the vicinity of theoretical molecular weight. In addition, the variations of polydispersity index (PDI) and $\frac{M_z}{M_w}$ are also computed during the course of the polymerization. Finally, molecular weight distributions (including number and weight distributions) have been calculated at different conversion.

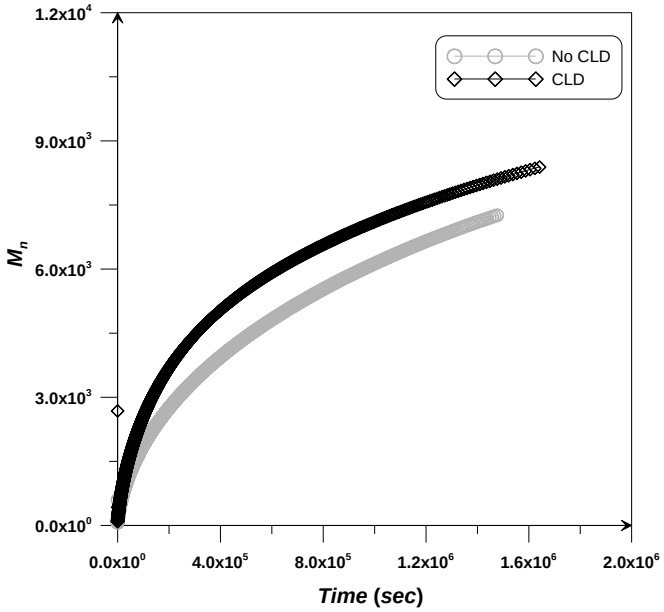

Fig. 8. Illustration of the dependence of number-average molecular weight on reaction time.

Fig. 9 depicts the augmentation of weight-average molecular weight during the polymerization reaction. Similar to number-average molecular weight, the weight-average molecular weight increases more sharply at the early stages of the polymerization. It is also deduced that the molecular weight of chains produced under conditions of chain-length-dependent termination reaction is larger than that of chains generated through the polymerization system in which the effect of chain length on termination reaction is neglected.

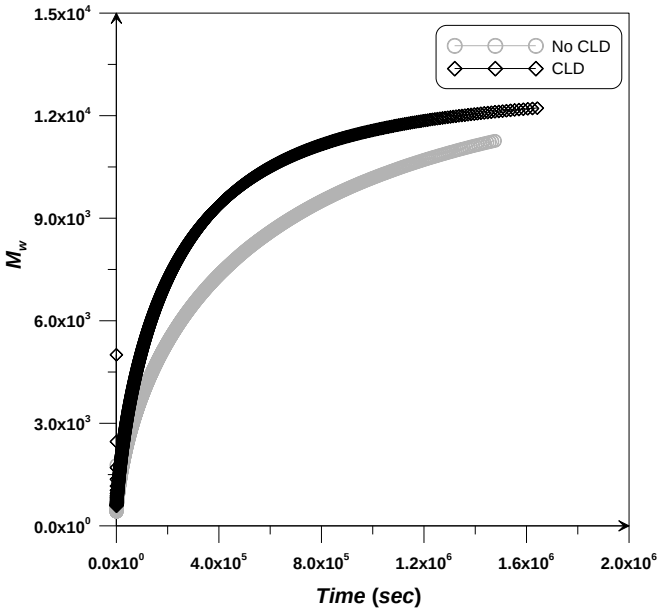

Fig. 9. Illustration of the dependence of weight-average molecular weight on reaction time.

The growth of z-average molecular weight is illustrated in Fig. 10. As expected, z-average molecular weight also ascends the same as M_n and M_w. However, at the final stages of the polymerization, as the concentration of monomer is becoming lower and lower, the z-average molecular weight of chains produced in the “CLD” case tends to plateau, while chains generated in the “No CLD” case continue growing.

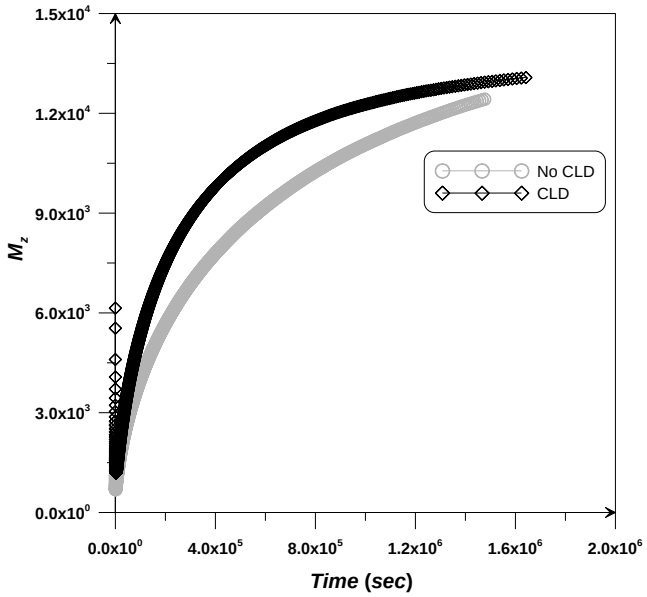

Fig. 10. Illustration of the dependence of z-average molecular weight on reaction time.

In other words, the z-average molecular weight of polymers produced without considering the effect of chain length on termination reaction, i.e. “No CLD” case, will probably become larger than that of polymers produced in the “CLD” case at the end of the polymerization. A slighter change can also be seen in weight-average molecular weight; however, it is not noticeable in the variation of number-average molecular weight. Therefore, it can be deduced that the predomination of molecular weight—weight- and especially z-average molecular weight—in the “No CLD” case at the final stages of the polymerization is because of termination by combination and coupling of chains, which affects the weight- and z-average molecular weights more remarkably than number-average molecular weight in the reaction time range studied. In fact, the effect of coupling reactions on M_w and M_z, rather than M_n, appears in lower conversion, as they are correspondingly influenced by the square and the cube of chain length.

As can be seen in Fig. 11, polydispersity index of polymer produced in ATRP greatly drops over the course of the polymerization. In fact, as the reaction proceeds, chains become more similar in length. In addition, it is shown that the decrease in polydispersity index continues to the very end of the polymerization. As presented in the inset of Fig. 11, it can been seen that the polydispersity index of polymers generated under conditions of applying chain length effect on the termination rate constant, namely the “CLD case”, is notably smaller than that of polymers produced without considering the effect of chain length on termination rate constant, i.e. the “No CLD” case, when the reaction progresses to high conversion.

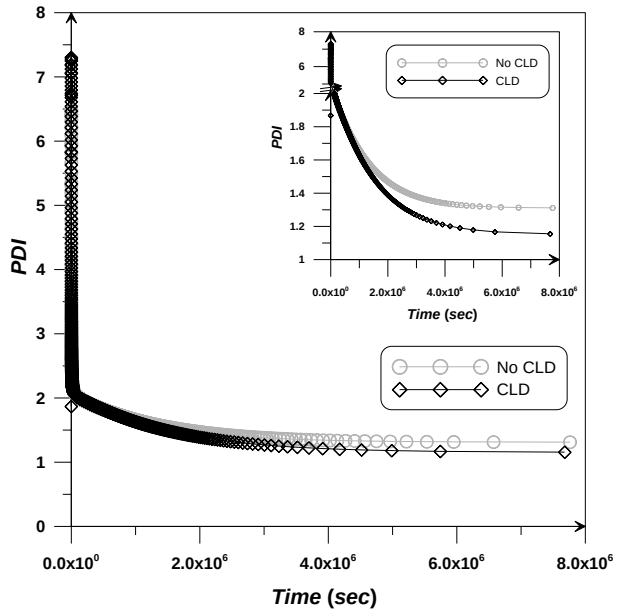

Fig. 11. Illustration of the dependence of polydispersity index on reaction time.

According to Fig. 12, similar to polydispersity index, $\frac{M_z}{M_w}$ falls throughout the polymerization. Nevertheless, as can be seen in the inset of Fig. 12, $\frac{M_z}{M_w}$ slightly increases during the later stages of the polymerization. This can be ascribed to a marked increase in z-average molecular weight; the sharper rise in $\frac{M_z}{M_w}$ in the "No CLD" case also corroborates this deduction, since z-average molecular weight increases more notably than weight-average molecular weight in the "No CLD" case as discussed above.

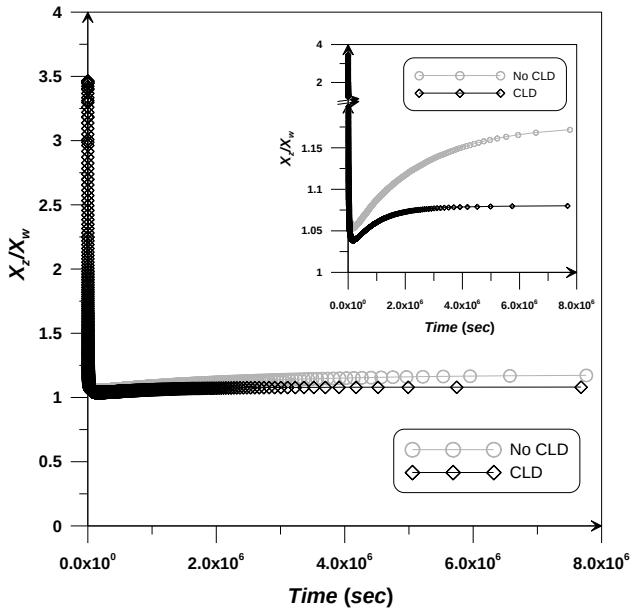

Fig. 12. Illustration of the dependence of $\frac{M_z}{M_w}$ on reaction time.

Simulating Complete Molecular Weight Distribution throughout Polymerization

Monte Carlo method, contrary to many analytical models, is able to easily calculate the molecular weight distributions during the polymerization as it is not dependent on solving some stiff, time-related differential equations. As mentioned above, the number and weight distributions of polymer chains are also plotted as a function of polymerization conversion and logarithmic scale of degree of polymerization (see Fig. 13 and Fig. 14). It can be noticed that the location of the peaks of both number and weight distributions shifts to higher molecular weight while the polymerization proceeds; in fact, this additionally affirms the feature of controlled/"living" radical polymerization, in which molecular weight linearly increases throughout the polymerization. Furthermore, it should be noted that both number and weight molecular weight distributions broaden at higher monomer conversion because of the accumulation of dead chains in the reactor.

In addition, when the chain-length-dependent termination rate constant is applied to the simulation program, two main features affirming the livingness of the system stand out: firstly, the reaction proceeds to higher conversion, i.e. 98.5% in the "CLD" case; secondly, the molecular weight distributions become narrower in comparison with the "No CLD" case (compare distributions having black vertical drop lines at 98.5% conversion with distributions having gray vertical drop lines at 86% conversion in Fig. 13 and Fig. 14).

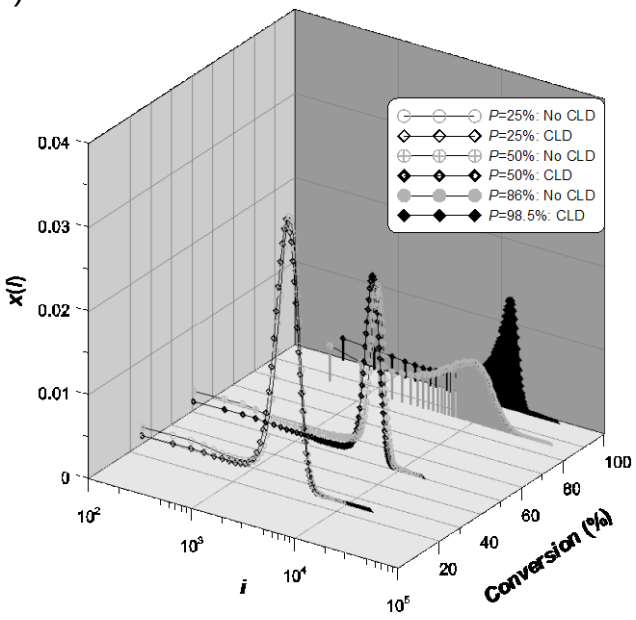

Fig. 13. Evolution of number-distribution throughout polymerization reaction.

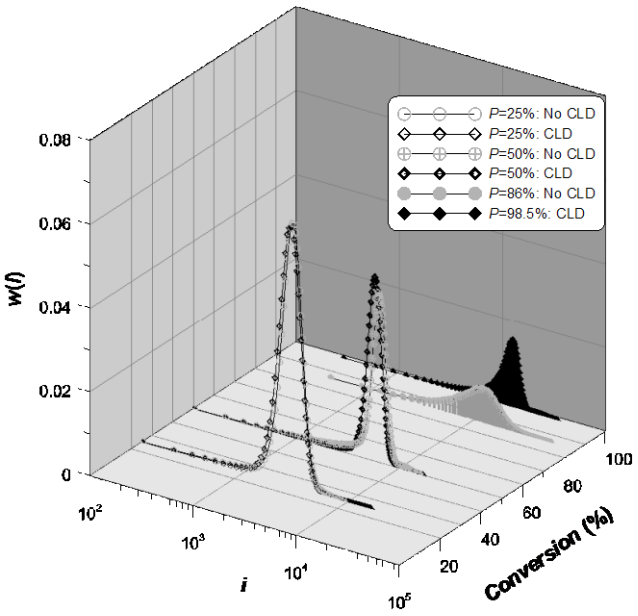

Fig. 14. Evolution of weight-distribution throughout polymerization reaction.

Conclusions

An optimized and high-performance Monte Carlo simulation is developed to thoroughly simulate the effect of chain length on bimolecular termination rate constant and correspondingly on the polymer microstructure in controlled/"living" radical polymerization by atom transfer. Simulation results show that termination rate constant greatly decreases over the course of the polymerization when it is chain-length dependent. The linear plot of $ln\left(\frac{M_0}{M}\right)$ against reaction time proves the livingness of the polymerization and shows that the reaction reaches higher conversion when the termination rate constant is chain-length dependent. In addition, as the plot of C_I against time shows, the initiator is decomposed at the early stages of the polymerization. The concentration of catalyst in higher oxidation state rises at first and then levels out at higher conversion. Furthermore, the amount of $X\text{-}M_t^{n+1}Y/L$ generated in the polymerization is lower when the chain-length-dependent termination rate constant is applied to the simulation. Also, the molecular weight of polymers produced through termination reactions with no chain-length dependency is smaller than when the termination reaction rate constant is chain-length dependent. Finally, the peak of molecular weight distribution of polymer chains shifts toward higher molecular weight throughout the polymerization. Besides, the molecular weight distributions become wider at the end of the polymerization. However, chain-length-dependent termination reactions result in narrower molecular weight distributions, as expected.

Acknowledgements

We wish to thank Ms. Ghazal Assadi-pour for her assistance with revising the language of this manuscript and her invaluable cooperation in the optimization of the simulation program.

References

[1] Goto, A.; Fukuda, T. *Prog*. *Polym*. *Sci*., **2004**, *29*, 329.
[2] Georges, M. K.; Veregin, R. P. N.; Kazmaier, P. M.; Hamer, G. K. *Macromolecules*, **1993**, *26*, 2987.
[3] Matyjaszewski, K.; Gaynor, S.; Wang, J. S. *Macromolecules*, **1995**, *28*, 2093.
[4] Kato, M.; Kamigaito, M.; Sawamoto, M.; Higashimura, T. *Macromolecules*, **1995**, *28*, 1721.
[5] Wang, J. S.; Matyjaszewski, K. *J*. *Am*. *Chem*. *Soc*., **1995**, *117*, 5614.
[6] Chiefari, J.; Chong, Y. K.; Ercole, F.; Krstina, J.; Jeffery, J.; Le, T. P. T.;
[7] Mayadunne, R. T. A.; Meijs, G. F.; Moad, C. L.; Moad, G.; Rizzardo, E.; Thang, S. H. *Macromolecules*, **1998**, *31*, 5559.
[8] Fischer, H. *J*. *Am*. *Chem*. *Soc*., **1986**, *108*, 3925.
[9] Georges, M. K.; Veregin, R. P. N.; Kazmaier, P. M.; Hamer, G. K. *Macromolecules*, **1993**, *26*, 2987.
[10] Benoit, D.; Chaplinski, V.; Braslau, R.; Hawker, C. J. *J*. *Am*. *Chem*. *Soc*., **1999**, *121*, 3904.
[11] Rodlert, M.; Harth, E.; Rees, I.; Hawker, C. J. *J*. *Polym*. *Sci*., *Polym*. *Chem*. *Ed*., **2000**, *38*, 4749.
[12] Feldermann, A.; Toy, A. A.; Phan, H.; Stenzel, M. H.; Davis, T. P.; Barner-Kowollik, C. *Polymer*, **2004**, *45*, 3997.
[13] Moad, G.; Chiefari, J.; Chong, Y. K.; Krstina, J.; Mayadunne, R. T. A.; Postma, A.; Rizzardo, E.; Thang, S. H. *Polym*. *Int*., **2000**, *49*, 993.
[14] Matyjaszewski, K.; Xia, J. *Chem*. *Rev*., **2001**, *101*, 2921.
[15] Kamigaito, M.; Ando, T.; Sawamoto, M. *Chem*. *Rev*., **2001**, *101*, 3689.
[16] Zhu, S. *J*. *Polym*. *Sci*., *Part B: Polym*. *Phys*., **1999**, *37*, 2692.
[17] Zhu, S. *Macromol*. *Theory Simul*., **1999**, *8*, 29.
[18] Delgadillo-Velazquez, O.; Vivaldo-Lima, E.; Quintero-Ortega, I.; Zhu, S. *AIChE J*., **2002**, *48*, 2597.
[19] Al-Harthi, M.; Soares, J. B. P.; Simon, L. *Macromol*. *Theory Simul*., **2006**, *15*, 198.
[20] Al-Harthi, M.; Soares, J. B. P.; Simon, L. *Macromol*. *Chem*. *Phys*., **2006**, *207*, 469.
[21] Wang, A.; Zhu, S. *J*. *Polym*. *Sci*., *Part A: Polym*. *Chem*., **2003**, *41*, 1553.
[22] Zhang, M.; Ray, H. *J*. *Appl*. *Polym*. *Sci*., **2002**, *86*, 1630.
[23] Zhang, M.; Ray, H. *J*. *Appl*. *Polym*. *Sci*. **2002**, *86*, 1047.
[24] Zhang, M.; Ray, H. *Ind*. *Eng*. *Chem*. *Res*., **2001**, *40*, 4336.
[25] Bonilla, J.; Saldivar, E.; Flores-Tlacuahuac, A.; Vivaldo-Lima, E.; Pfaendner, R.; Tiscareno-Lechuga, F. *Polym*. *React*. *Eng*., **2002**, *10*, 227.
[26] Greszta, D.; Matyjaszewski, K. *Macromolecules*, **1996**, *29*, 7661.
[27] Shipp, A.; Matyjaszewski, K. *Macromolecules*, **1999**, *32*, 2948.
[28] Shipp, A.; Matyjaszewski, K. *Macromolecules*, **2000**, *33*, 1553.
[29] Lutz, J.; Matyjaszewski, K. *Macromol*. *Chem*. *Phys*., **2002**, *203*, 1385.
[30] Barner-Kowollik, C.; Quinn, J. F.; Morsley, D. R.; Davis, T. P. *J*. *Polym*. *Sci*., *Polym*. *Chem*. *Ed*., **2001**, *39*, 1353.
[31] Chaffey-Millar, H.; Busch, M.; Davis, T. P.; Stenzel, M. H.; Barner-Kowollik, C. *Macromol*. *Theory Simul*., **2005**, *14*, 143.
[32] Mohammadi, Y.; Najafi, M.; Haddadi-Asl, V. *Macromol*. *Theory Simul*., **2005**, *14*, 325.

[33] Najafi, M.; Haddadi-Asl, V.; Mohammadi, Y. *J Appl. Polym. Sci*., **2007**, *106*, 4138.
[34] He, J.; Zhang, H. D.; Yang, Y. *Macromol*. *Theory Simul*., **1995**, *4*, 811.
[35] Tobita, H. *Macromol*. *Theory Simul*., **2003**, *12*, 32.
[36] He, J.; Zhang, H.; Yang, Y. *Macromol*. *Theory Simul*., **1993**, *2*, 747.
[37] He, J.; Li, L.; Yang, Y. *Macromol*. *Theory Simul*., **2000**, *9*, 463.
[38] He, J.; Zhang, H.; Chen, J.; Yang, Y. *Macromolecules*, **1997**, *30*, 8010.
[39] Al-Harthi, M.; Soares, J. B. P.; Simon, L. C. *Macromol. React. Eng.*, **2007**, *1*, 468.
[40] Al-Harthi, M.; Soares, J. B. P.; Simon, L. *Macromol*. *Mat*. *Eng*., **2006**, *291*, 993.
[41] Tobita, H. *Macromol*. *Theory Simul*., **2006**, *15*, 23.
[42] Al-Harthi, M.; Soares, J. B. P.; Simon, L. C. *Macromol*. *React*. *Eng*., **2007**, *1*, 95.
[43] Kwark, Y. J.; Novak, B. M. *Macromolecules*, **2004**, *37*, 9395.
[44] Queffelec, J.; Gaynor, S. G.; Matyjaszewski, K. *Macromolecules*, **2000**, *33*, 8629.
[45] Fu, Y.; Hutchinson, R. A.; Cunningham, M. F. *Macromol*. *React*. *Eng*., **2007**, *1*, 243.
[46] Ohno, K.; Goto, A.; Fukuda,T.; Xia, J.; Matyjaszewski, K. *Macromolecules*, **1998**, *31*, 2699.
[47] Matyjaszewski, K.; Davis, K.; Patten, T.; Wei, M. *Tetrahedron*, **1997**, *53*, 15321.
[48] Olaj, O. F.; Vana, P. *Macromol*. *Rapid Commun*., **1998**, *19*, 433.
[49] Olaj, O. F.; Vana, P. *Macromol*. *Rapid Commun*., **1998**, *19*, 533.
[50] Olaj, O. F.; Vana, P.; Kornherr, A.; Zifferer, G. *Macromol*. *Chem*. *Phys*., **1999**, *200*, 2031.
[51] Buback, M.; Egorov, M.; Junkers, T.; Panchenko, E. *Macromol*. *Rapid Commun*., **2004**, *25*, 1004.
[52] Smith, G. B.; Russell, G. T.; Heuts, J. P. A. *Macromol*. *Theory Simul*., **2003**, *12*, 299.
[53] Gillespie, D. *J*. *Phys*. *Chem*., **1977**, *81*, 2340.